PAPER

Developments for pulsed antihydrogen production towards direct gravitational measurement on antimatter

IOP Publishing Physica Scripta
Phys. Scr. 95 (2020) 114001 (8pp) https://doi.org/10.1088/1402-4896/abbaa1

Developments for pulsed antihydrogen production towards direct gravitational measurement on antimatter

M Fanì[1,2,3,26], M Antonello[4,5], A Belov[6], G Bonomi[7,8], R S Brusa[9,10], M Caccia[4,5], A Camper[1], R Caravita[10], F Castelli[4,11], D Comparat[12], P Cheinet[12], G Consolati[4,13], A Demetrio[14], L Di Noto[2,3], M Doser[1], R Ferragut[4,15], J Fesel[1], S Gerber[1], M Giammarchi[4], A Gligorova[16], L T Glöggler[1], F Guatieri[9,10], S Haider[1], A Hinterberger[1], A Kellerbauer[25], O Khalidova[1], D Krasnicky`[2], V Lagomarsino[2,3], C Malbrunot[1], L Nowak[1], S Mariazzi[9,10], V Matveev[6,17], S R Müller[14], G Nebbia[18], P Nedelec[19], M Oberthaler[14], E Oswald[1], D Pagano[7,8], L Penasa[9,10], V Petracek[20], L Povolo[9,10], F Prelz[4], M Prevedelli[21], B Rienäcker[1], O M Røhne[23], A Rotondi[8,22], H Sandaker[23], R Santoro[4,5], G Testera[2], I C Tietje[1], V Toso[4,15], T Wolz[1], C Zimmer[1,14,23] and N Zurlo[24]

[1] Physics Department, CERN, 1211 Geneva 23, Switzerland
[2] INFN Genova, via Dodecaneso 33, 16146 Genova, Italy
[3] Department of Physics, University of Genova, via Dodecaneso 33, 16146 Genova, Italy
[4] INFN Milano, via Celoria 16, 20133 Milano, Italy
[5] Department of Science, University of Insubria, Via Valleggio 11, 22100 Como, Italy
[6] Institute for Nuclear Research of the Russian Academy of Science, Moscow 117312, Russia
[7] Department of Mechanical and Industrial Engineering, University of Brescia, via Branze 38, 25123 Brescia, Italy
[8] INFN Pavia, via Bassi 6, 27100 Pavia, Italy
[9] Department of Physics, University of Trento, via Sommarive 14, 38123 Povo, Trento, Italy
[10] TIFPA/INFN Trento, via Sommarive 14, 38123 Povo, Trento, Italy
[11] Department of Physics 'Aldo Pontremoli', University of Milano, via Celoria 16, 20133 Milano, Italy
[12] Université Paris-Saclay, CNRS, Laboratoire Aimé Cotton, 91405, Orsay, France
[13] Department of Aerospace Science and Technology, Politecnico di Milano, via La Masa 34, 20156 Milano, Italy
[14] Kirchhoff Institute for Physics, Heidelberg University, Im Neuenheimer Feld 227, 69120 Heidelberg, Germany
[15] LNESS, Department of Physics, Politecnico di Milano, via Anzani 42, 22100 Como, Italy
[16] Stefan Meyer Institute for Subatomic Physics, Austrian Academy of Sciences, Boltzmanngasse 3, 1090 Vienna, Austria
[17] Joint Institute for Nuclear Research, Dubna 141980, Russia
[18] INFN Padova, via Marzolo 8, 35131 Padova, Italy
[19] Institute of Nuclear Physics, CNRS/IN2p3, University of Lyon 1, 69622 Villeurbanne, France
[20] Czech Technical University, Prague, Brehová 7, 11519 Prague 1, Czech Republic
[21] University of Bologna, Viale Berti Pichat 6/2, 40126 Bologna, Italy
[22] Department of Physics, University of Pavia, via Bassi 6, 27100 Pavia, Italy
[23] Department of Physics, University of Oslo, Sem Sælandsvei 24, 0371 Oslo, Norway
[24] Department of Civil, Environmental, Architectural Engineering and Mathematics, University of Brescia, via Branze 43, 25123 Brescia, Italy
[25] Max Planck Institute for Nuclear Physics, Saupfercheckweg 1, 69117 Heidelberg, Germany

E-mail: mattia.fani@cern.ch

[26] Currently at Los Alamos National Laboratory, P.O. Box 1663 Los Alamos, NM 87545.

0031-8949/20/114001+08$33.00

Received 1 April 2020, revised 27 August 2020
Accepted for publication 22 September 2020
Published 5 October 2020

Abstract

A main scientific goal of the AEgIS experiment is the direct measurement of the Earth's local gravitational acceleration g on antihydrogen. The Weak Equivalence Principle is a foundation of General Relativity. It has been extensively tested with ordinary matter but very little is known about the gravitational interaction between matter and antimatter. Antihydrogen is produced in AEgIS via resonant charge-exchange reaction between cold Rydberg-excited positronium and cooled down antiprotons. The achievements for the development of a pulsed cold antihydrogen source are presented. Large number of antiprotons, necessary for a significant production rate of antihydrogen, are captured, accumulated, compressed and cooled over an extended period of time. Positronium (Ps) is formed through e^+-Ps conversion in a silica porous target at 10 K temperature in a reflection geometry inside the main apparatus. The so-formed Ps cloud is then laser-excited to Rydberg levels, for the first time in a 1 T magnetic field. Consequently, a detailed characterization of the Ps source for antihydrogen production in magnetic field needed to be performed. Several detection techniques are extensively used to monitor antiproton and positron manipulations in the formation process of antihydrogen inside the main apparatus. Positronium detection techniques underwent extensive improvements in sensitivity during the last antiproton run. At the same time, major efforts to improve integrate and commission the detectors sensitive to antihydrogen production took place.

Keywords: antimatter, gravity, antihydrogen, antiproton, positronium

(Some figures may appear in colour only in the online journal)

1. Introduction

AEgIS (Antimatter Experiment: gravity, Interferometry, Spectroscopy) [1] is an experiment presently running at CERN's Antiproton Decelerator (AD) facility. One of its primary goals consists in performing a direct test of the validity of the Weak Equivalence Principle (WEP) on neutral antimatter systems by measuring the Earth gravitational acceleration g on a beam of cold antihydrogen. Unlike all the other antihydrogen experiments performed or in progress at the AD [2–6], $\bar{H}$ is formed in AEgIS through charge-exchange reaction between cold antiprotons and a cloud of Rydberg-excited positronium atoms (Ps^*). The method was first demonstrated in [7] with a different technique.

After a brief introduction to the production scheme of antihydrogen in AEgIS in section 2, the final protocol of antiproton manipulations for antihydrogen production will be described in section 3. The procedure, finalised during the last antiproton run, allows large numbers of antiprotons, necessary for a significant production rate of antihydrogen, to be captured, accumulated, compressed and cooled over an extended period of time. An overview of the techniques developed for the detection of charged particles, excited states of positronium in magnetic field and antihydrogen is finally given in section 4. With geometrical limitations and in the presence of a strong magnetic field, the detection of excited states of positronium in the production region required the development of a novel imaging technique with the use of a micro-channel plate detector. Finally, an outline of the two detectors sensitive to antihydrogen production will be provided in section 4.2.

2. Antihydrogen in the AEgIS experiment

Antihydrogen ($\bar{H}$) is the bound state of an antiproton ($\bar{p}$) and a positron (e^+). Ps^* is obtained by a two-steps excitation of positronium (Ps). Positronium is a purely leptonic hydrogen-like bound state of an electron and its antiparticle, the positron. In AEgIS, Ps is produced by the conversion of a positron bunch hitting a nano-porous target. The picture in figure 1 outlines the antihydrogen formation process and the subsequent gravity measurement. Once produced, the antihydrogen has to be horizontally conveyed into a Stark-accelerated beam towards a grating system which includes time and position detectors. The g value will be obtained by measuring the vertical displacement of velocity selected populations of antiatoms flying through a two-grating system. The expected precision is at %-level using sub-Kelvin antihydrogen and a grating system operated in the classical regime (moirè deflectometer). Higher accuracy could be obtained by using colder antihydrogen and quantum interferometers. The module for the gravity measurement has to be implemented in the experimental apparatus. In addition, a discussion about possible future upgrades of the experiment is currently ongoing.

Antiprotons are only available at the CERN's Antiproton Decelerator (AD) at energies feasible for manipulations. This aspect makes the ADthe only place in the world where study of fundamental physics with cold antimatter can be performed. Antimatter experiments need high magnetic fields and electromagnetic trap systems to manipulate charged particles and non-neutral plasmas. To manipulate antiprotons for antihydrogen production, AEgIS uses a two-stage

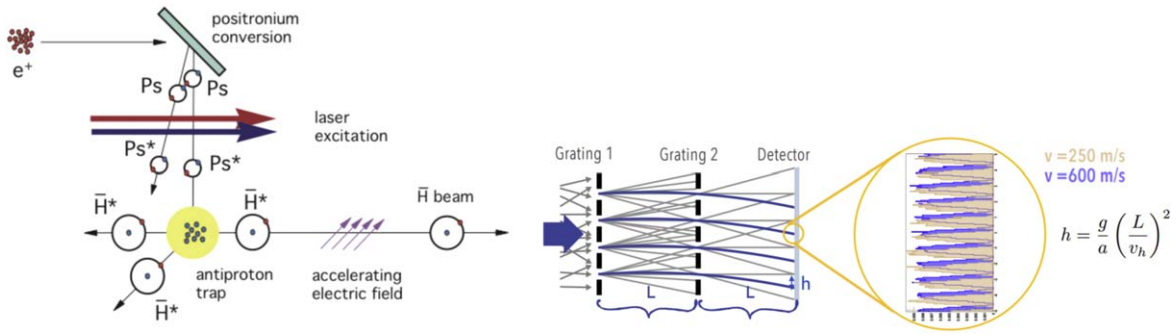

Figure 1. Outline of the antihydrogen formation process and gravity measurement. Illustration adapted from [8].

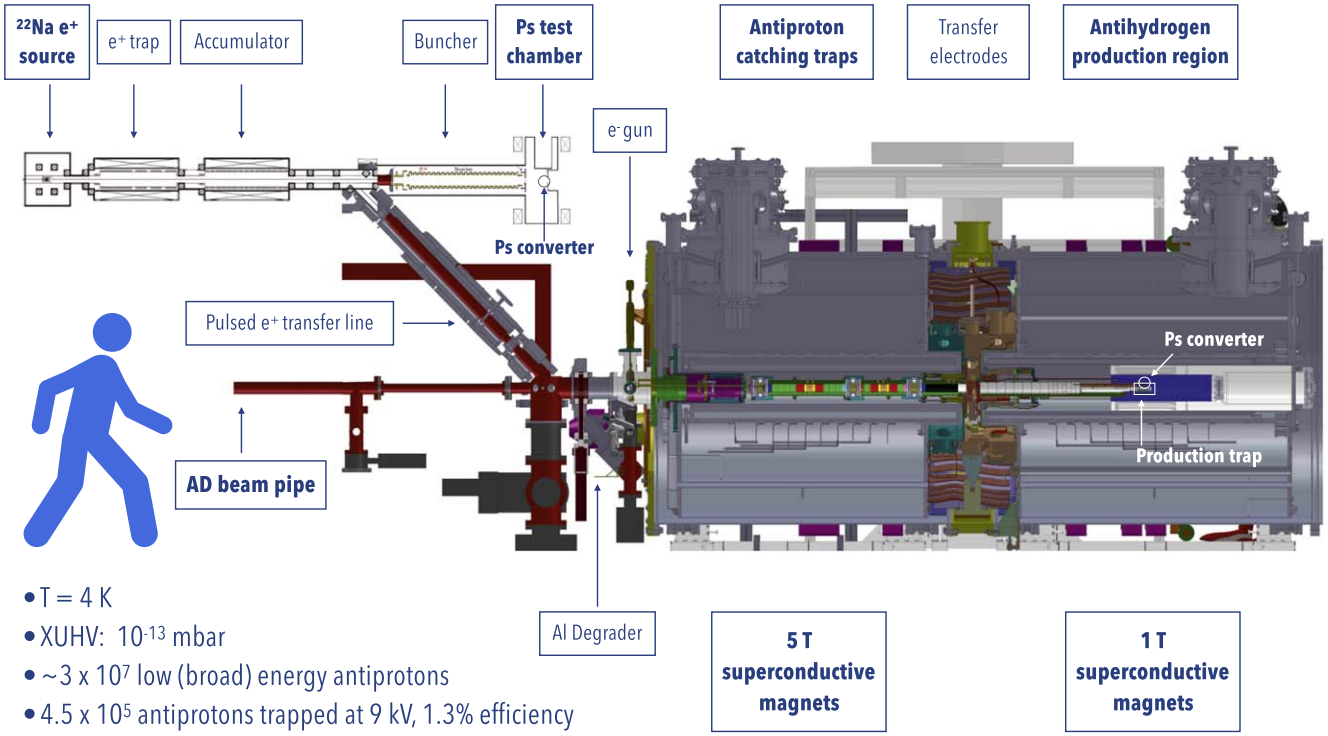

Figure 2. Overview of the AEgIS experimental apparatus. Antiprotons arrive from the ADbeam pipe on the left of the picture. Then, they are captured, compressed and cooled in the following stages of the apparatus. Positrons are emitted by the sodium source in the top left corner and conveyed towards the positronium converter inside the main apparatus. The antihydrogen production reaction takes place in the 1T region.

Penning-Malmberg trap immersed in a 5 T and a 1 T magnetic fields and contained in a single cryogenic and ultra-high vacuum cryostat. Figure 2 gives an overview of the AEgIS experimental apparatus. Capture, compression and a first stage of the cooling process are performed in the 5T region. More refined procedures aimed to antihydrogen production take place in the 1T region.

3. Antiproton manipulations for antihydrogen formation

AEgIS receives antiprotons from ADat 5.3 MeV (100 MeV/c) in bunches of variable length (from 200 to 500 ns), containing $\sim 3 \cdot 10^7$ $\bar{p}$ each [9]. The ADinjection energy exceeds the energy of trappable particles by two orders of magnitude. AEgIS captures about $4 \cdot 10^5$ $\bar{p}$ per ADshot with energies up to 10 keV using a multiple layer beam degrader (in total 170 μm of aluminium and 55 μm of silicon) for the first deceleration stage. As of 2021, with the Extra Low Energy Antiproton ring (ELENA) in operation at the ADfacility, there is the potential to improve capture efficiency of one order of magnitude.

Once captured, the antiprotons have to be driven into the production trap to wait for the arrival of the Rydberg Ps cloud in suitable condition for efficient antihydrogen production. An energy of 10^{-2} eV or less can be reached in the $\bar{H}^{Prod}_{Trap}$ for macroscopic times with the antiproton plasma in good compression conditions. The overall procedure is composed of several steps which were sequentially developed, commissioned and optimised over the past few years and finalised for efficient production during the last antiproton run, in 2018.

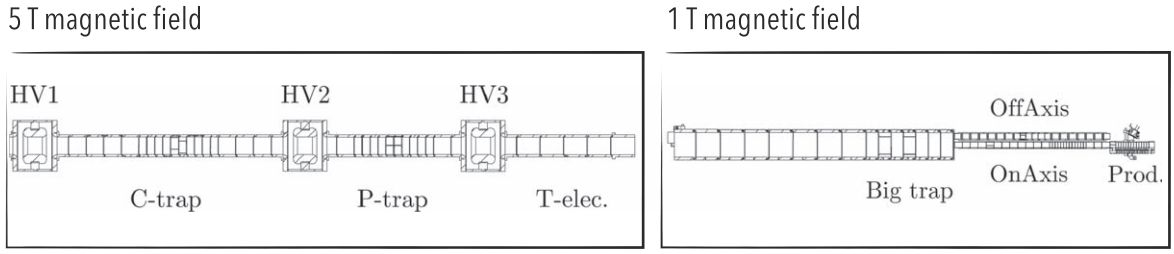

Figure 3. Overview of the Penning-Malmberg trap system in AEgIS. The connection to the ADis upstream the HV1 electronde. The two trap regions reside in two separate sections of the cryostat.

The major advance was the full implementation of the anti-hydrogen formation procedure with an increased production rate as a result of improvements on plasma conditions and an enhanced production efficiency due to the introduction of a multi-stacking technique.

Figure 3 gives an overview of the AEgIS trap system. Antiproton trapping is performed at the entrance of the 5T traps using a trap of about 35 cm length, 1.5 cm radius, the C-trap. A 9 kV high-voltage is applied to the end electrodes of the capture trap with a voltage rise time of $\sim$10 ns. Trapped antiprotons need to be cooled down and compressed before being transferred to the 1T traps for further manipulations to prepare them for efficient charge-exchange reaction. A first cooling stage takes place in the capture trap. Then, the antiprotons are moved to the P-trap for compression. A different approach would involve electrodes from both C- and P-traps for capture, and the P trap electrodes only for compression, after a potential well reshaping.

A first round of sympathetic cooling is carried out through collisions with a preloaded electron plasma at the capture time. The technique is now well-established and allows the trapped antiprotons to decrease their energy to the eV level. The electron trap is 3 cm long and the resulting electron density is in the order of 10^8 e^- cm^{-3}. The number of electrons is then reduced by 40 V steps of the potential wells and the trap is adiabatically reshaped to a flat Malmberg trap with its bottom level at 140 V. At the arrival of the ADshot, the antiprotons are captured in a physical region surrounding the electron trap and start losing energy by collision. After a few tens of seconds, the *hottest* $\bar{p}$ fraction is dumped by lowering one of the trap edges. The resulting annihilation signal is monitored and recorded as an on-line reference of the number of antiprotons trapped. The remaining fraction, the 90% of those initially trapped, is moved into the compression trap. Interestingly, a considerable fraction of antiprotons are trapped at large radii inside the trap. They can be cooled if the electron plasma reaches a suitably large radial distribution.

Before being transferred to the production trap, the antiproton plasma has to be compressed to compensate for the natural expansion due to the two different field strengths and to favour longer storage times in the $\bar{H}$ production trap. In addition, a good compression prevents the plasma from significant losses during the transfer. This is motivated by two reasons. Firstly, the 5T and 1T traps are intrinsically misaligned. In the second place, the magnetic field abruptly drops to 0.8 T in the transfer region, resulting in an even more significant expansion between the two magnets. Another argument for $\bar{p}$ plasma compression resides in the design constraints of the production region. The ability to compress antiproton clouds to small radii allows for a radially small $\bar{H}$ production trap. As the converter target has to be mounted externally to trap electrodes, a good plasma compression, ultimately, results in a reduction of the distance between the $e^+$to Ps target and the antiproton cloud, with a consequent increase of the reaction efficiency. Finally, driving antiproton clouds into the production trap already with a small radius helps tackling the radial expansion issues induced by the non-standard design of the $\bar{H}$ production trap. A multi-step compression method was developed, based on the application of the *rotating wall* technique, with progressive reduction of the number of electrons. Details can be found in [10]. A ten-fold radial compression of antiproton plasma has been achieved, with a typical radius of 0.17 mm only for the single ADbunch, in the 5T trap.

Compressed antiproton clouds are *ballistically* transferred from the 5T to the 1T traps. The procedure consists of four main steps: opening the P-trap towards the transfer region, moving the potentials to favour the cloud shift, in-flight centring of the antiprotons and recapturing them in the 1T traps. The in-flight centring is done with the application of a controlled shift of the radial position of the antiproton cloud by setting static voltages ranging from -180 to $+180$ V to the 4 radial sectors of one cylindrical electrode mounted in transition region between the two magnets.

Once in the 1T trap, the antiproton cloud is recaptured in the production trap. It is a Malmberg-Penning trap composed of 15 electrodes with 5 mm radius and mounted 10 mm below the Ps converter target. A schematic of the production trap is sketched in figure 4. Due to the need for an entrance for the laser-excited Ps, the central electrodes of the production trap have a 2 mm wide opening on their top to let Ps atoms fly in towards the $\bar{p}$ cloud. As any opening in the electrode walls is known to produce electric field distortions, the slits are covered by a 80%-transparent honeycomb geometry mesh designed to minimise the field distortions due to the opening. Residual field distortions, however, severely affect the plasma stability in the trap reducing the storage time.

Cooling of the antiprotons recaptured in the $\bar{H}_{Trap}$ requires electrons. In the final procedure, first the antiprotons are ballistically captured in the designated trap and then the electrons are captured in the same trap, again ballistically,

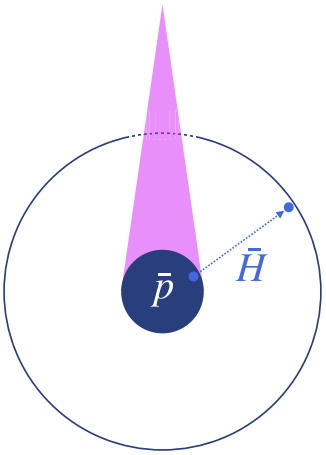

Figure 4. Cross-section view of the AEgIS production trap, composed of 15 electrodes. Central electrodes, here represented, have an open slit on their top to allow the Ps atoms to fly in. Antihydrogen atoms are produced via charge-exchange reaction with the antiprotons.

from the reservoir B-trap. About $\sim 2 \cdot 10^7$ electrons are captured in the selected antiproton trap by lowering the potentials on the upstream electrodes for such a short time as to prevent significant losses of antiprotons. Then the electrodes are again pulsed up to the previous potentials so that the trap shape is restored within 40 ns of the opening time. Once the initial cooling stage is completed, a large fraction of the electrons are dumped by applying fast, short pulses to one electrode as to prevent the electron space-charge potential from influencing the temperature measurement. The remaining electrons continue to cool antiprotons for a second cooling stage of 10 seconds. Electrons and antiprotons are then moved adiabatically into a different region of the $\bar{H}_{Trap}$ with a better overlap with the Rydberg positronium for the antihydrogen formation experiments.

A multi-stack procedure was developed during the last antiproton run, in 2018. It consists of capture and storing several antiproton bunches from AD. Once the hottest fraction of particles in the plasma is removed, it is possible to capture another antiproton bunch, sympathetically cool it down with the plasma already trapped and release again the most energetic particles while waiting for the next shot. In principle, this procedure can be endlessly repeated and a great number of shots can be stored in the 5T traps. However, a good compromise between the number of stored antiprotons and the plasma expansion in the production trap was found with the stacking of 8 ADshots. Notably, this corresponds to a number of antiprotons per $\bar{H}$ production trial about 10 times larger than expected in the original AEgIS proposal [11]. The resulting plasma, containing up to $\sim 10^6$ antiprotons, could be stored for several thousands of seconds in the production trap in stable conditions without any further manipulation.

The possibility to store antiprotons in the production trap for such a long time gave the opportunity to run multiple cycles of antihydrogen production with the same $\bar{p}$ cloud. An $\bar{H}$ production cycle corresponds to a Ps formation process. In typical conditions, positrons are accumulated, compressed and sent to the target converter every $\sim 90 - 100$ seconds. A fraction of formed Ps cloud is then laser-excited to Rydberg states and enters the production trap to interact with the $\bar{p}$ cloud. Figure 5 shows the comparison between the radial profile of a mixed $\bar{p}$-e^- plasma in typical conditions for $\bar{H}$ production. The picture displays electron images. The antiproton distribution follows that of the electrons. The radial profile of an 8 ADshots plasma stored for 20 $\bar{H}$ cycles expanded to ~ 2 mm only in more than half an hour. Antiproton losses have been observed due to unavoidable collisions with residual gas. A fraction of about $\simeq 75\%$ of the initial number of antiprotons is still measured after more than 3000 seconds with a negligible plasma expansion and this can be considered an estimation of the maximum losses due to collisions with residual gas. Occasionally, larger losses related to plasma dynamics and correlated with larger antiproton radial size were observed, most probably caused by the fluctuating conditions of the electron cloud stored in the 1 T production trap together with the antiprotons. The pulsed production procedure can operate for up to 50 production cycles, which corresponds to 75 minutes without significant antiproton losses or significant radial expansion. Under standard conditions, a production procedure of 24 cycles guaranteed a good compromise between reliability and efficiency.

4. Detection of excited states of Ps and $\bar{H}$ in the production region

4.1. Positronium diagnostics in 1T

Positronium is the intermediate system to produce antihydrogen via charge-exchange reaction with antiprotons in AEgIS. Its long-lived fraction corresponding to the triplet spin configuration, *ortho*-Ps, has a decay constant of 142 ns. Laser-excitation to higher levels extends the Ps lifetime. In addition, the cross-section of the charge-exchange reaction scales with the fourth power of the Ps principal quantum number. In AEgIS, the Ps laser excitation to Rydberg states is performed in two steps. First, the $n_{Ps} = 3$ level is reached by means of a broadband UV laser pulse with 205.045 nm wavelength, 1.5 ns duration and $\sim 40\,\mu$J energy. Then, a second synchronized broadband IR laser is used, with pulses 3 ns long, and wavelength tunable from 1680 to 1720nm, 1.6 mJ energy for the subsequent excitation to Rydberg levels. The presence of the magnetic field, needed for antiproton manipulations, affects the energy levels of Ps atoms. The excited positronium atoms are distributed in energy around that of the $n_{Ps} = 17$ level that would have been reached in the absence of a magnetic field, with n_{Ps} ranging in the interval 14-22. Rydberg-excited positronium clouds enter into the $\bar{H}_{Trap}$ while cold antiproton plasmas are stored in suitable conditions for antihydrogen production. The time when the laser is fired is the reference time for the pulsed production scheme and it is known with a few ns accuracy.

Figure 6 shows the $\bar{H}$ production region where positrons reach the target converter to generate a Ps cloud. Downstream

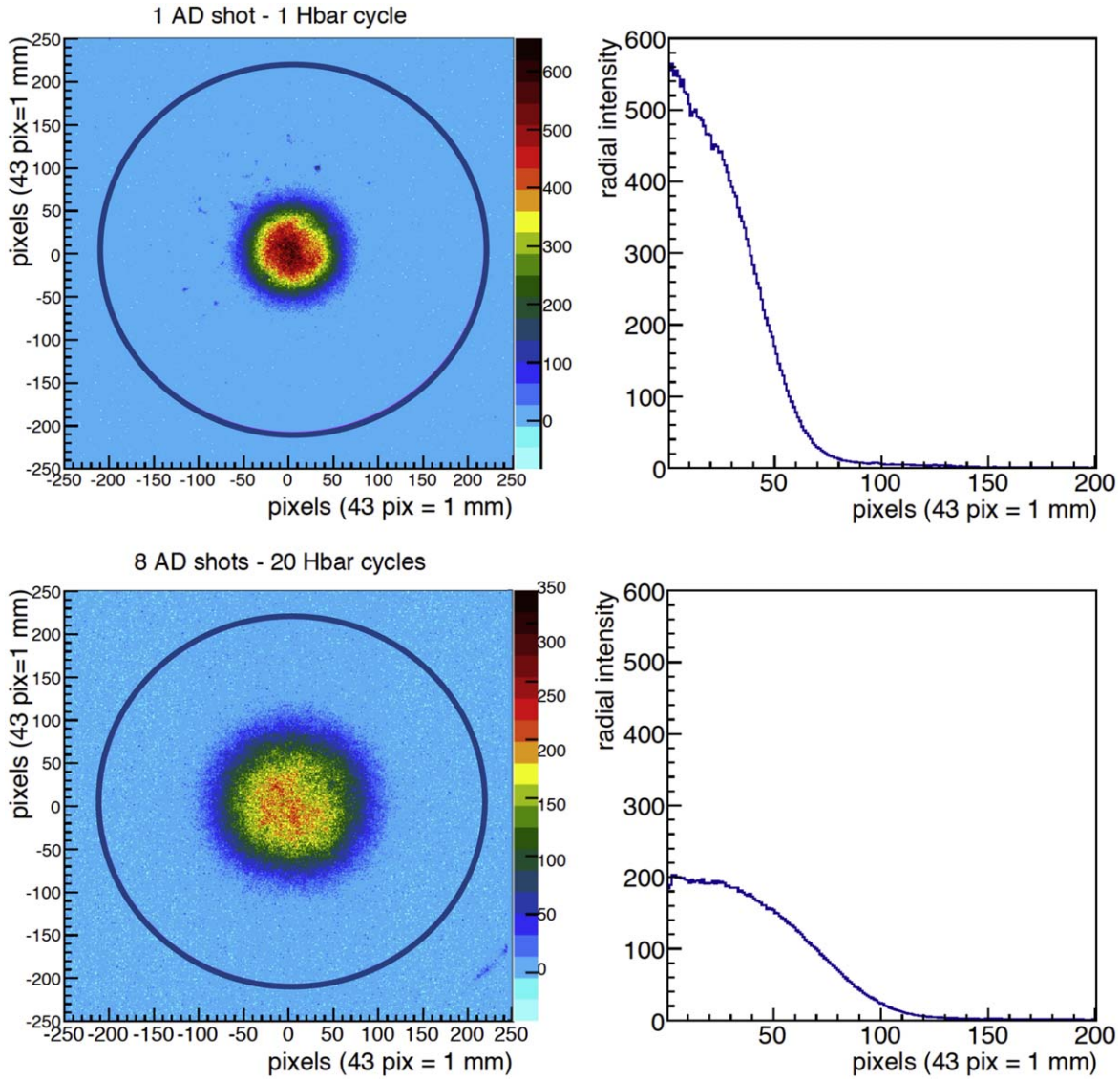

Figure 5. Electrons released from the antihydrogen production trap to the MCP downstream the trap system. The circles indicate the trap inner profile. On the top: electrons needed to compress a single ADshot plasma stored for one production cycle only. On the bottom: electrons for a 8 ADshots plasma stored for about half an hour. MCP image is reported on the left side of each row, radial profile distribution on the right side. Antiproton distribution follows that of electrons.

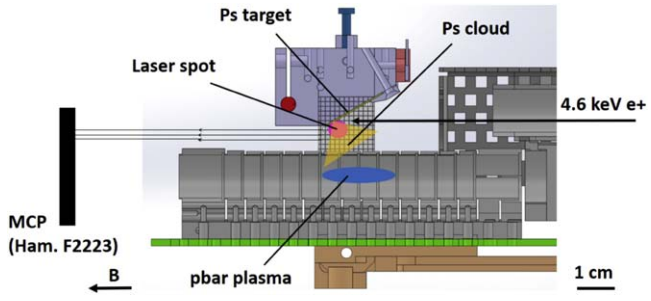

Figure 6. Detail of the AEgIS $\bar{H}$ production region. A fraction of the Ps is laser-excited to Ps^* to reach the $\bar{p}$ plasma waiting inside the production trap at cold temperature in conditions suitable for antihydrogen formation via charge exchange reaction. The picture is taken from [12].

the end of the trap system, at the far left of the figure, a dual-readout Hamamatsu F2223 MCP/phosphor screen assembly is placed for $\bar{p}$ plasma diagnostics. After the 2018 upgrade, the Ps target holder structure was moved a few millimetres upwards to allow the Ps flight path to be visible from the MCP.

A fast and reliable detection method for slow positronium was developed on the basis of the simultaneous acquisition of a semi-cylindrical wide-area plastic scintillation detector (see section 4.2) surrounding the AEgIS cryostat and the MCP assembly installed in the $\bar{H}$ production region. The technique is compatible with the cryogenic 1T magnetic field environment necessary for handling antiproton plasmas and allows to fully overcome the stringent limitations imposed by the environmental requirements to standard techniques widely

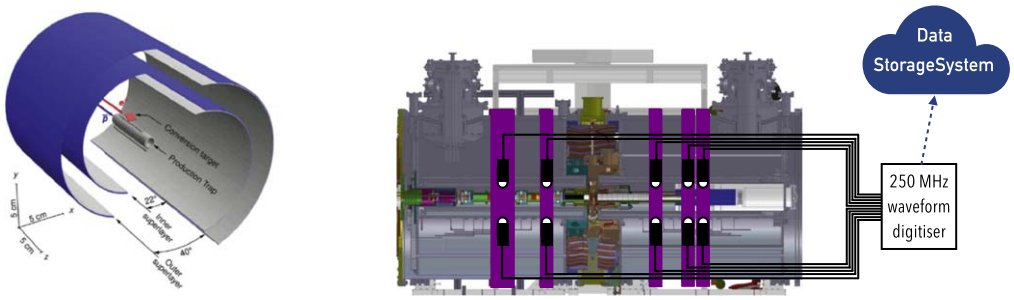

Figure 7. The antihydrogen dedicated detectors. Left panel: the FACT detector (picture taken from [16]). Right panel: the ESDA detector. Details are in the text.

adopted in the positron community. The idea behind the upgrade of positronium diagnostics is the repositioning of the target holder and consequently the target itself a few millimetres upwards. In doing so, the MCP has an enhanced field of vision. The Ps atoms are photo-ionized by a laser pulse and the detached positrons are collected by the MCP. The detection of such positrons by the MCP allows to image them and infer the information about position, velocity and evolution of the Ps cloud. The resolution of the produced picture is estimated in 10 μm. Either detached electrons or positrons are detected, depending on the MCP polarization. The particles reach the MCP keeping their position in the transverse plane as they are bound to their cyclotron orbits around the magnetic field lines which are perpendicular to the MCP's surface. Details on the experimental methodology developed are discussed in [12–14].

The Single Shot Positron Annihilation Lifetime Spectroscopy technique (SSPALS) is a well established technique commonly used to detect the Ps formation and variations in its lifetime spectra [15]. At the time of the Conference, the characterization of a new scintillating material for a possible future upgrade in the AEgIS detection system was ongoing. The laser-excitation of the ortho-Ps inducing slight distortions of the exponential decay curve, the detector must have a very rapid response, minimal afterglow and a wide angle coverage to allow direct measurements of the Ps clouds entering the production trap. Preliminary activities gave encouraging results in improvements of the sensitivity in the time region of interest for Ps^* studies.

4.2. Antihydrogen detectors

Detection of antihydrogen formation in AEgIS is the detection of the annihilation of an antiproton on the surface atomic layers of the trap electrodes. Annihilation processes can involve protons and neutrons of the material and typically result in the production of a number of charged pions.

The dedicated detector for antihydrogen annihilation is the Fast Annihilation Cryogenic Tracking detector (FACT, [16] - Figure 7, left). It is composed of 794 ring-shaped scintillating fibres (Kuraray SCSF-78 M) disposed in two concentric double-layer cylinders around the antihydrogen production trap at cryogenic temperature with an active region of about 300 mm in length. Each scintillating fibre is coupled to a plain fibre that conveys the scintillation light to a Multi-Pixel Photon Counter (MPPC) detector at the external flange of the experiment, at room temperature. Each fibre is monitored at 200 MHz and comparing the output of the silicon photomultiplier with a predefined threshold results in a purely digital hit map of all fibres with 5 ns temporal resolution. The passage of a particle through a fibre is recorded as two spatial coordinates and one temporal data. Tracks and vertexes have to be reconstructed from such information.

The AEgIS External Scintillator Detector Array (ESDA, [17] - Figure 8, right) consists of twelve general-purpose, fast plastic scintillator paddles made of commercial EJ-200 from Eljen Technology; each one is coupled to two photomultiplier tubes, one at each scintillator end. ESDA slabs externally surround the vacuum chamber for monitoring $\bar{p}$ and e^+annihilations and turned out to be a crucial tool for antihydrogen detection in 2018. Each scintillating slab is 1cm thick, ~150 cm long, and shaped to cover a 120° arc of the cryostat containing the superconducting magnet. The four scintillators surrounding the 5T traps are 20 cm wide while the eight surrounding the 1T traps are 10 cm wide for a better spatial resolution. Each 1T slab covers a solid angle of about 3% with respect to an annihilation happening in its center. The overall ESDA coverage around the antihydrogen production region is ~20% of 4π. Each slab is optically coupled to two independent heavily shielded photomultiplier tubes, typically counted in coincidence within a window of 50 ns for cleaner signals. Photomultiplier tubes used to acquire the scintillator slabs are EMI 9954B and Philips XP2020, with slightly different features between each other which, however, can be neglected for the AEgIS purposes. Among the 24 PMTs coupled to the external scintillators, those deputed to Ps studies are also acquired on a parallel acquisition chain using a fast 12 bit, 2 GS/s oscilloscope to diagnose positronium in the antihydrogen production region.

5. Conclusions

AEgIS is an experiment presently running at CERN's Antiproton Decelerator (AD) facility. Several classes of detectors are implemented in a wide range of techniques in the detection of charged particles, non-neutral plasmas, positronium and antihydrogen. Large number of antiprotons are captured, accumulated, compressed and cooled over an extended period of time. Antiprotons are compressed in a 5 T field down to

170 μm radii. The introduction of a stacking procedure significantly increased the efficiency of the overall antihydrogen production scheme. Positronium is formed and studied both in a dedicated setup and inside the main apparatus with a detailed characterization of the Ps source for antihydrogen production. A new diagnostics allowed a precise characterization of the travel path of the Ps cloud towards the antihydrogen production trap. A new scintillator-based innovative detector promises a better precision in the diagnostics of positronium measurements. At the time of the Conference, a preliminary data-analysis of production of antihydrogen was still ongoing. Results of further analyses have been submitted for publication.

ORCID iDs

M Fanì https://orcid.org/0000-0002-4284-9614
G Consolati https://orcid.org/0000-0003-3614-245X
R Ferragut https://orcid.org/0000-0002-6079-1831
S Gerber https://orcid.org/0000-0001-5101-1250
A Kellerbauer https://orcid.org/0000-0002-2755-1713
G Testera https://orcid.org/0000-0003-2970-766X

References

[1] Doser M *et al* (AEgIS Collaboration) 2018 AEgIS at ELENA: outlook for physics with a pulsed cold antihydrogen beam *Philos. Trans. R. Soc. Lond.* A **376** 20170274 10 p
[2] Amoretti M *et al* (ATHENA Collaboration) 2002 Production and detection of cold antihydrogen atoms *Nature* **419** 456–9
[3] Gabrielse G *et al* (ATRAP Collaboration) 2002 Background-free observation of cold antihydrogen with field-ionization analysis of its states *Phys. Rev. Lett.* **89** 213401
[4] Andresen G B *et al* (ALPHA Collaboration) 2010 Trapped antihydrogen *Nature* **468** 673–6
[5] Enomoto Y *et al* (ASACUSA Collaboration) 2010 Synthesis of cold antihydrogen in a cusp trap *Phys. Rev. Lett.* **105** 243401
[6] Perez P and Sacquin Y 2012 The GBAR experiment: gravitational behaviour of antihydrogen at rest *Classical Quantum Gravity* **29** 184008
[7] Storry C H(ATRAP Collaboration) *et al* 2004 First laser-controlled antihydrogen production *Phys. Rev. Lett.* **93** 1–4 https://link.aps.org/doi/10.1103/PhysRevLett.93.263401
[8] Doser M *et al* (AEgIS Collaboration) 2011 Measuring the fall of antihydrogen: the AEgIS experiment at CERN *Phys. Proc.* **17** 49–56 2nd International Workshop on the Physics of fundamental Symmetries and Interactions—PSI2010
[9] Maury S 1997 The antiproton decelerator: AD *Hyperfine Interact.* **109** 43–52
[10] Aghion S *et al* (AEgIS Collaboration) 2018 Compression of a mixed antiproton and electron non-neutral plasma to high densities *Eur. Phys. J.* D **72** 76
[11] Drobychev G(AEgIS Collaboration) *et al* 2007 Proposal for the AEGIS experiment at the CERN antiproton decelerator (Antimatter Experiment: Gravity, Interferometry, Spectroscopy) *Technical Report* CERN-SPSC-2007-017. SPSC-P-334, CERN, Geneva https://cds.cern.ch/record/1037532
[12] Caravita R *et al* (AEgIS Collaboration) 2019 *AIP Conf. Proc.* **2182** 030002
[13] Amsler C *et al* (AEgIS Collaboration) 2019 A $\sim$100 μm-resolution position-sensitive detector for slow positronium *Nucl. Instrum. Meth.* B **457** 44–8
[14] Camper A *et al* (AEgIS Collaboration) 2019 Imaging a positronium cloud in a 1 Tesla *EPJ Web Conf.* **198** 00004
[15] Cassidy D B *et al* 2006 Single shot positron annihilation lifetime spectroscopy *Appl. Phys. Lett.* **88** 194105
[16] Amsler C *et al* (AEgIS Collaboration) 2020 A cryogenic tracking detector for antihydrogen detection in the AEgIS experiment *Nucl. Instrum. Methods Phys. Res., Sect. A* **960** 163637
[17] Zurlo N *et al* (AEgIS Collaboration) 2020 Calibration and equalisation of plastic scintillator detectors for antiproton annihilation identification over positron/positronium *In: ed. by Acta Physica Polonica* B **51** 213–23